

Detection of gravitational waves through pulsar observations

Alexander Rodin

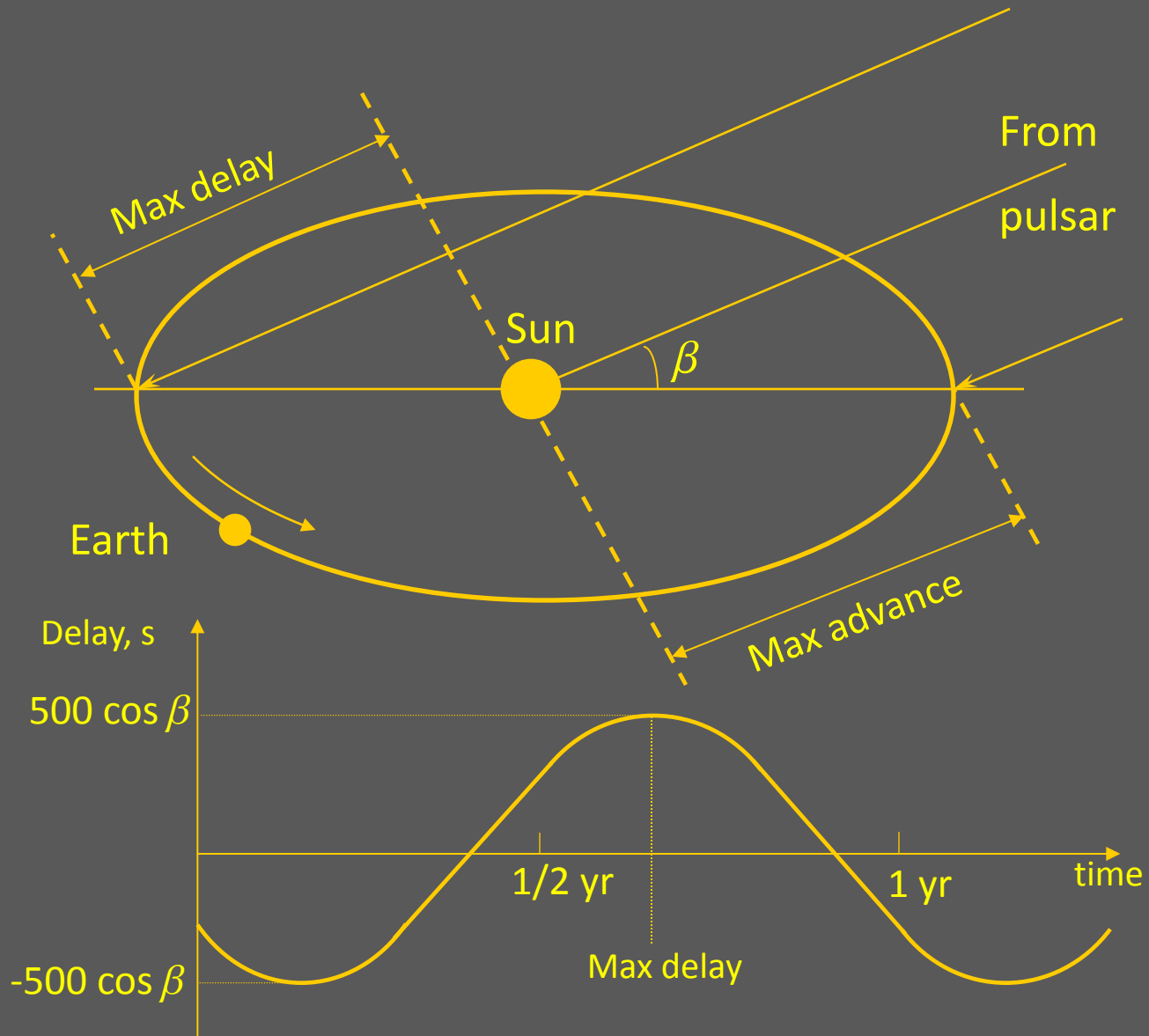
(rodin@prao.ru)

Lebedev Physical Institute
Russian Academy of Sciences

Plan of lecture

- Pulsar timing
- Pulsar time scale and upper limit of the GWB
- Observations
- Data processing (SSA)
- Pulsar timing array and principle of GW detection
- Discussion

Pulsar timing



Pulsar timing

$$c(t' - t) = -\vec{k} \cdot \vec{r} + \frac{1}{2R} [\vec{k} \times \vec{r}]^2 + \delta t_{rel} + \frac{DM}{2.41 \cdot 10^{-16}} \frac{1}{f_{obs}^2} + \delta t_h,$$

Diagram illustrating the components of the pulsar timing equation:

- Pulsar unit vector** (\vec{k})
- Observer radius-vector** (\vec{r})
- Shapiro delay** (δt_{rel})
- Dispersion measure** ($DM = \int_0^R n_e dl$)
- observed time** (t')
- calculated time** (t)
- Pulsar distance** (R)
- Observational frequency** (f_{obs})

$$t = t_0 + P_0 N + \frac{1}{2} P_0 \dot{P} N^2 - \text{time of arrival of } N\text{th pulse to the Solar system barycenter}$$

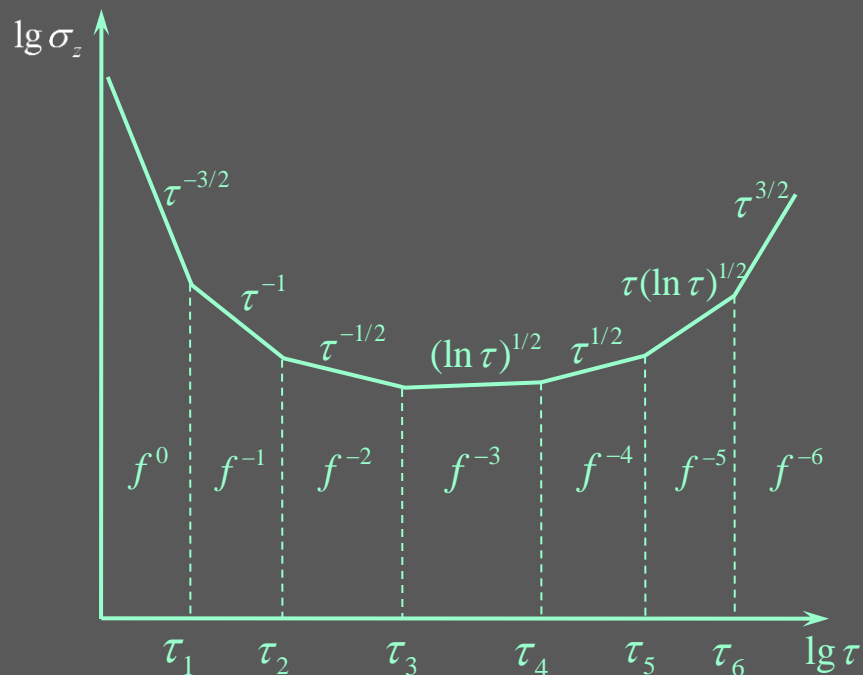
t_0 – initial epoch,

P_0, \dot{P} – pulsar spin period and derivative,

N – pulse number.

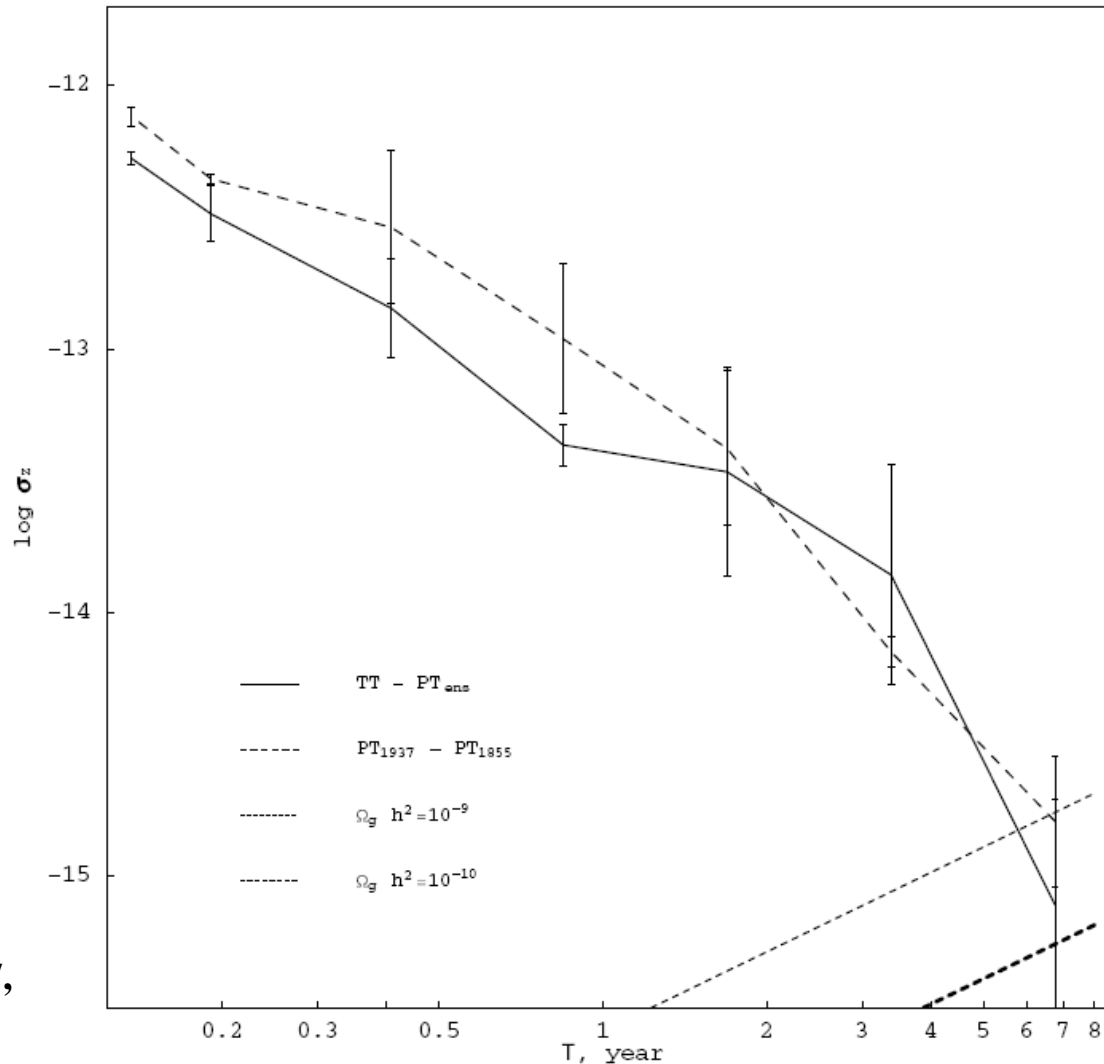
Pulsar time scale

Behavior of the fractional instability σ_z in dependence on observation interval τ and kind of noise (Ilyasov, Kopeikin, Rodin, *The astronomical timescale based on the orbital motion of a pulsar in a binary system*, 1998, Ast.Lett, 24, 228).



Spectral index k	Kind of noise	Reference
0	Instrumental errors	Yu.Ilyasov, S.Kopeikin, A.Rodin, 1998, Astr. Lett, 24, 228
-1	Flicker in phase	Ibid.
-2	Random walk in phase	R. Blandford, R. Narayan, R. Romani, <i>J. Astroph. Astron</i> , 5 , 369 (1984).
-3	Interstellar medium (flicker in frequency)	Ibid., J.Armstrong, <i>Nature</i> , 307 , 527 (1984)
-4	Random walk in frequency	
-5	Primordial GW background	B. Bertotti, B.J. Carr, M.J. Rees, <i>MNRAS</i> , 203 , 945 (1983).
-6	Random walk in torque (freq. deriv.)	

Pulsar time scale



A.Rodin, MNRAS, **387**,
1583–1588 (2008)

Figure 5. The fractional instability σ_z based on the difference $PT_{1937} - PT_{1855}$ (dashed line) and σ_z of the difference $TT - PT_{\text{ens}}$ (solid line). Theoretical values of σ_z in the cases $\Omega_g h^2 = 10^{-9}$ and 10^{-10} are shown in the lower right-hand corner of the plot.

Observations



Radio telescope: RT-64 (~170 km North from Moscow).

Pulsar receiver: AS-600.

Frequency: 610 MHz, B=2 x 3.2 MHz.

A total of 6 millisecond pulsars (5 binary):

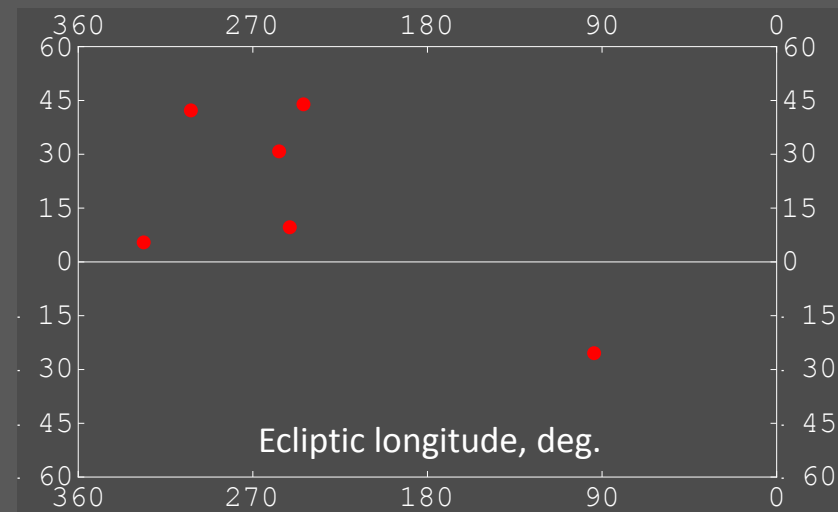
J0613-0200, J1640+2224, J1643-1224,
J1713+0747, B1937+21, J2145-0750

Observations

Pulsar name	Spin period, ms	DM, $\text{cm}^{-3} \cdot \text{pc}$	Binary period, days	RMS, mcs	Instrum. error, mcs
J0613-0200	3.062	38.78	1.2	14.8	0.30
J1640+2224	3.163	18.42	175.46	5.4	0.17
J1643-1224	4.622	62.41	147.02	11.6	0.47
J1713+0747	4.570	15.99	67.83	10.5	0.16
B1937+21	1.558	71.04	-	2.2	0.53
J2145-0750	16.052	9.00	6.84	14.9	0.12

Pulsar timing observations were carried out with 64 m radio telescope of Kalyazin radio astronomy observatory (KRAO) at frequency 610 MHz in bandwidth 2 x 3.2 MHz (Oreshko.V.V., *Pulsar timing instrumental errors. AC-600/1600 facility*. Proceedings of the Lebedev Physical Institute., Moscow, 2000, v. 229, p. 110 (*in Russian*)).

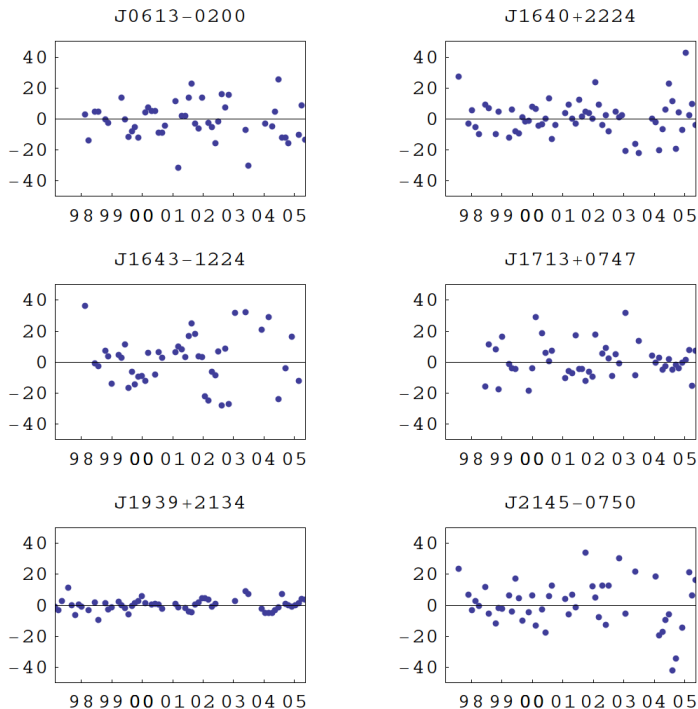
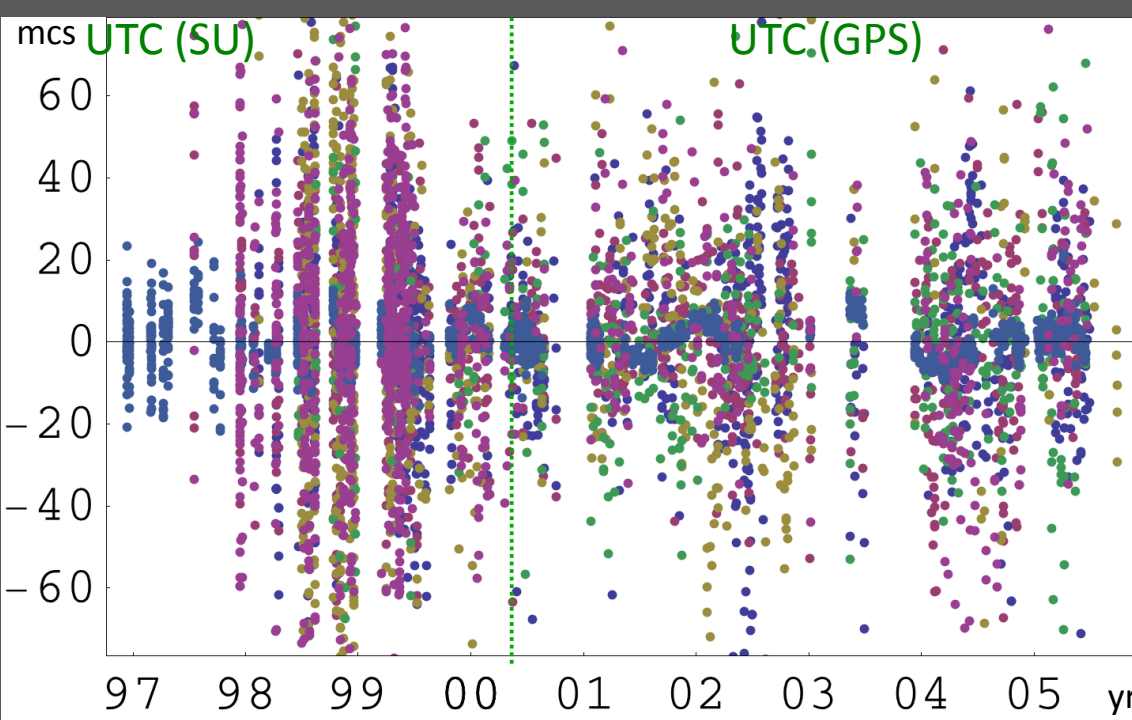
Distribution of pulsars on the sky



Observations

Barycentric post-fit timing residuals of 6 millisecond pulsars.

(Ilyasov, Y. P.; Oreshko, V. V.; Potapov, V. A.; Rodin, A. E. 2004, IAUS, **218**, 433)



Averaged post-fit timing residuals (length 51 points) of 6 millisecond pulsars. Averaging interval 40 days. Gaps were filled by linear interpolation.

Data processing

(Singular Spectrum Analysis)

$$\{x_i\}_{i=1}^N = (x_1, x_2, \dots, x_N) \longrightarrow X = \begin{pmatrix} x_1 & x_2 & \dots & x_M \\ x_2 & x_3 & \dots & x_{M+1} \\ \vdots & \vdots & \ddots & \vdots \\ x_k & x_{k+1} & \dots & x_N \end{pmatrix} \longrightarrow R = XX^T$$

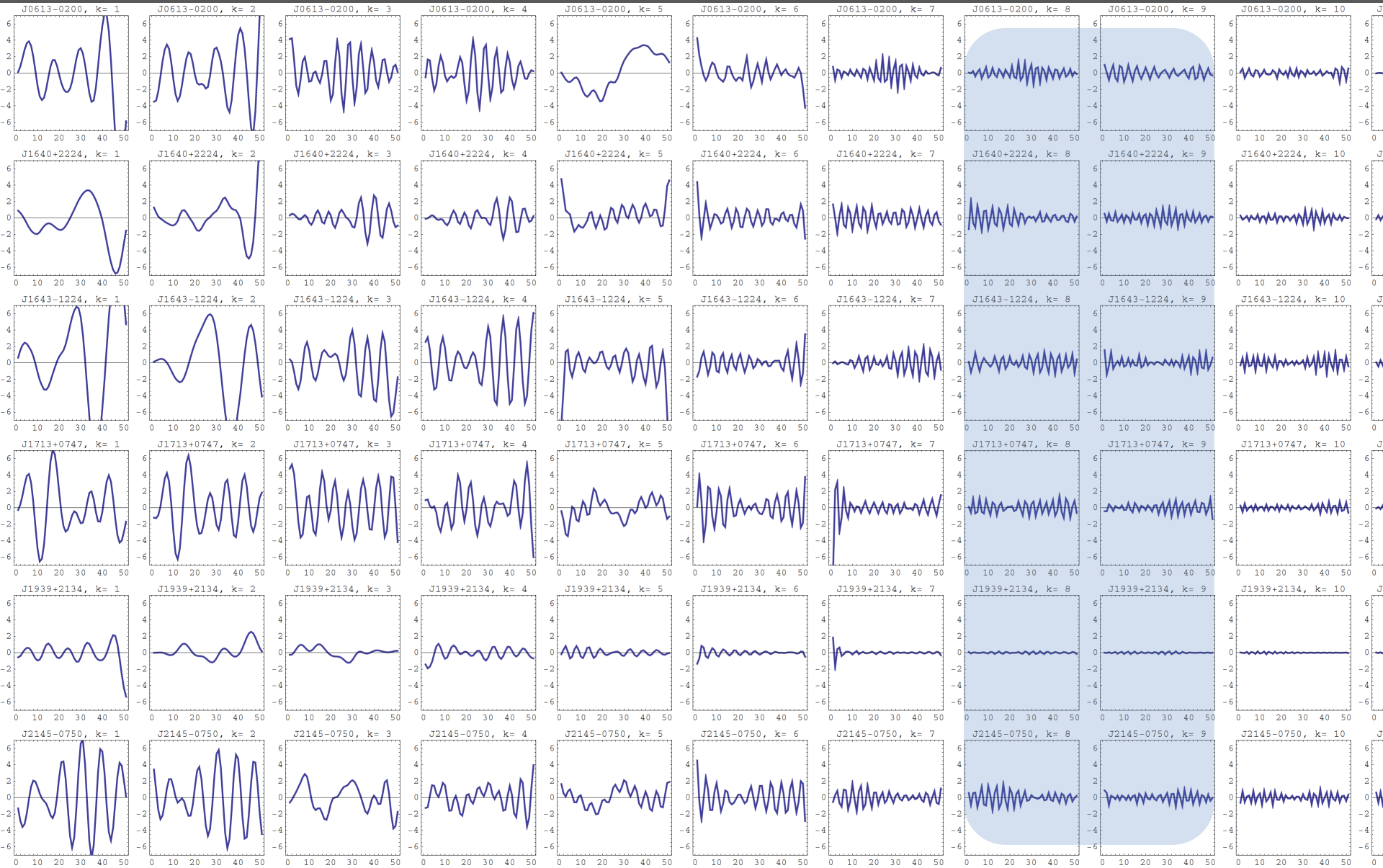
- covariance matrix;

$$\left\{ \begin{array}{l} R = P\Lambda P^T, \\ \Lambda = \begin{pmatrix} \lambda_1 & 0 & \dots & 0 \\ 0 & \lambda_2 & \dots & 0 \\ \vdots & \vdots & \ddots & \vdots \\ 0 & 0 & \dots & \lambda_M \end{pmatrix} \\ P = \begin{pmatrix} p_{11} & p_{21} & \dots & p_{M1} \\ p_{12} & p_{22} & \dots & p_{M2} \\ \vdots & \vdots & \ddots & \vdots \\ p_{1M} & p_{2M} & \dots & p_{MM} \end{pmatrix} \end{array} \right. \begin{array}{l} \text{- eigenvalue matrix;} \\ \text{- eigenvector matrix;} \end{array}$$

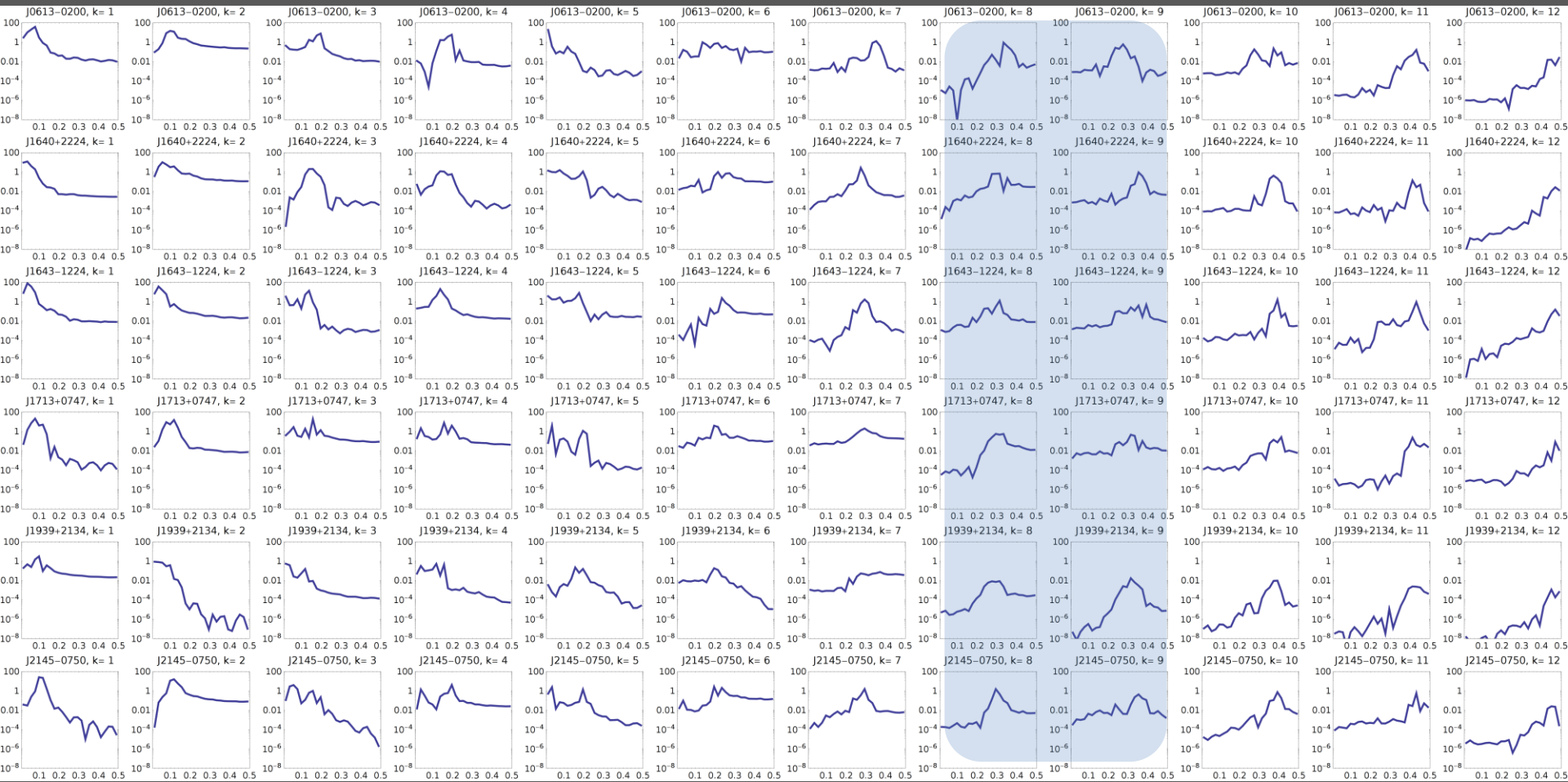
$$Y = PX \quad \text{- principal components matrix;}$$

$$\tilde{X} = Y' P^T \quad \text{- reconstructed matrix.}$$

Data processing



Data processing



Detection of gravitational waves

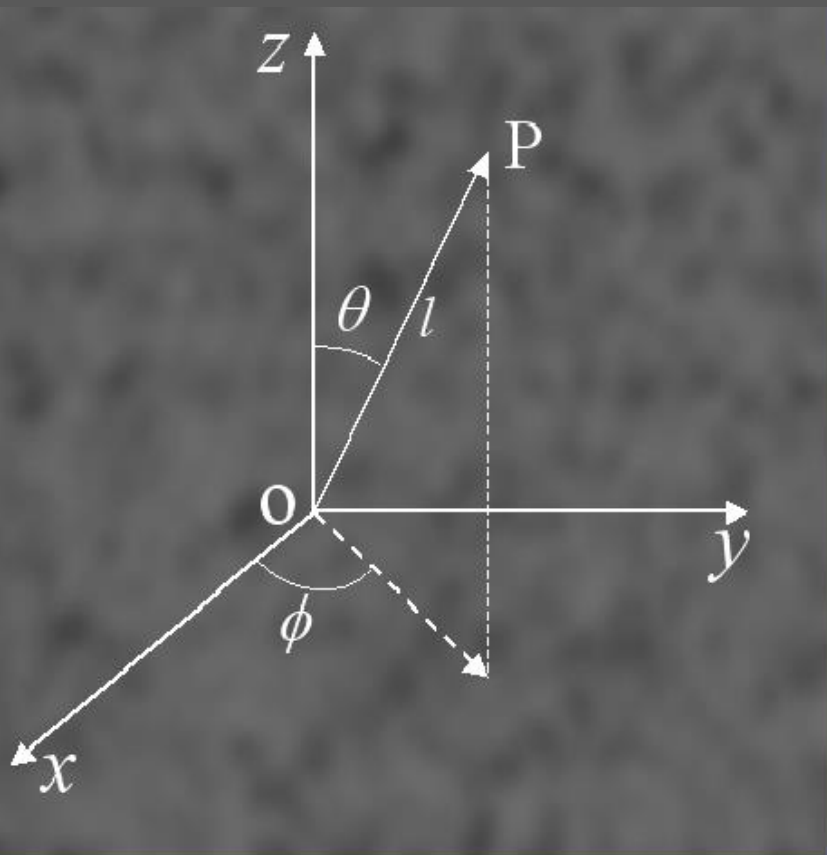
Fractional change of pulsar spin frequency due to propagation of GW:

$$\frac{\Delta\nu}{\nu} = \frac{1}{2} \cos 2\phi [1 - \cos \theta] \times (h(t) - h(t - l - l \cos \theta))$$

$h(t)$ – amplitude of the gravitational wave common to all pulsars,

(Eastabrook & Wahlquist 1975; Hellings & Downs 1983)

l – distance to pulsar P,



ϕ – angle between a principle polarization vector of the wave and projection of the pulsar position l on the transverse plane xOy ,

θ – angle between Earth-pulsar distance and the wave propagation direction (z -axis).

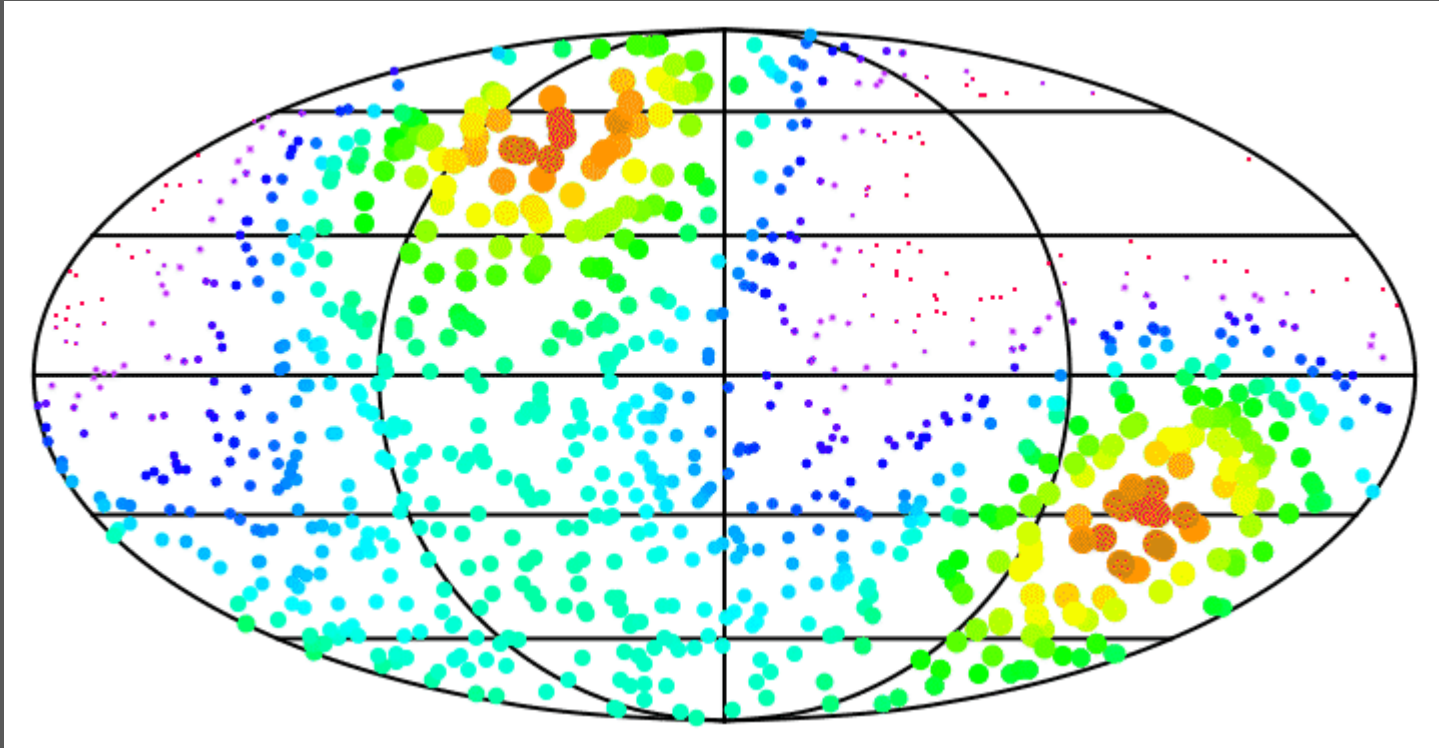
$C_{ij} = \alpha_{ij} \langle h^2 \rangle + \delta C_{ij}$, – two-point correlation

$$\alpha_{ij} \equiv \frac{1}{4} \int \alpha_i \alpha_j d\Omega = x \ln x - \frac{x}{6} + \frac{1 + \delta(x)}{3}, \quad x = \frac{1 - \cos \gamma}{2}.$$

(Hellings, Downs, 1983);

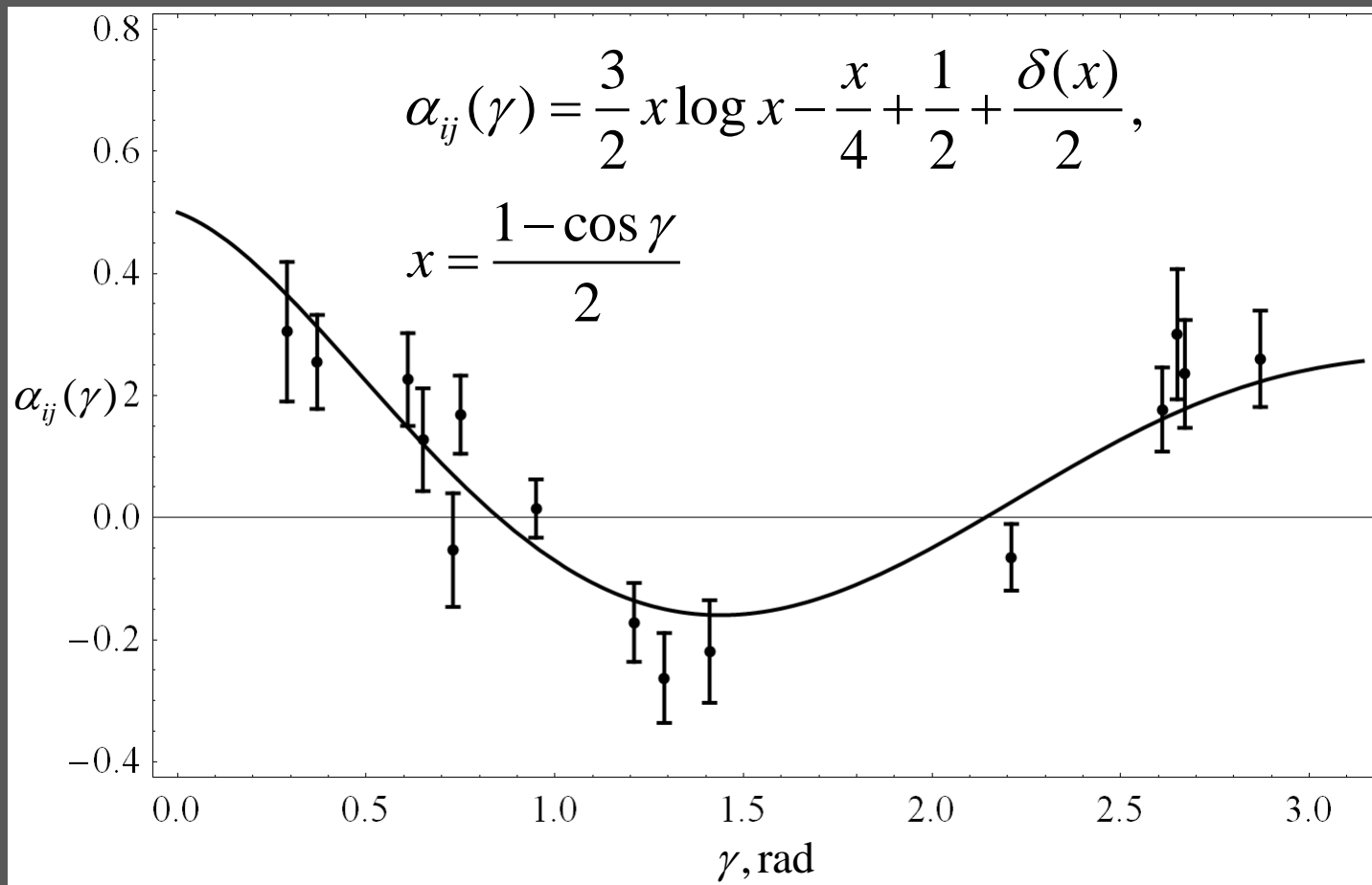
(Jenet, Hobbs, Lee and Manchester, 2005).

Detection of gravitational waves



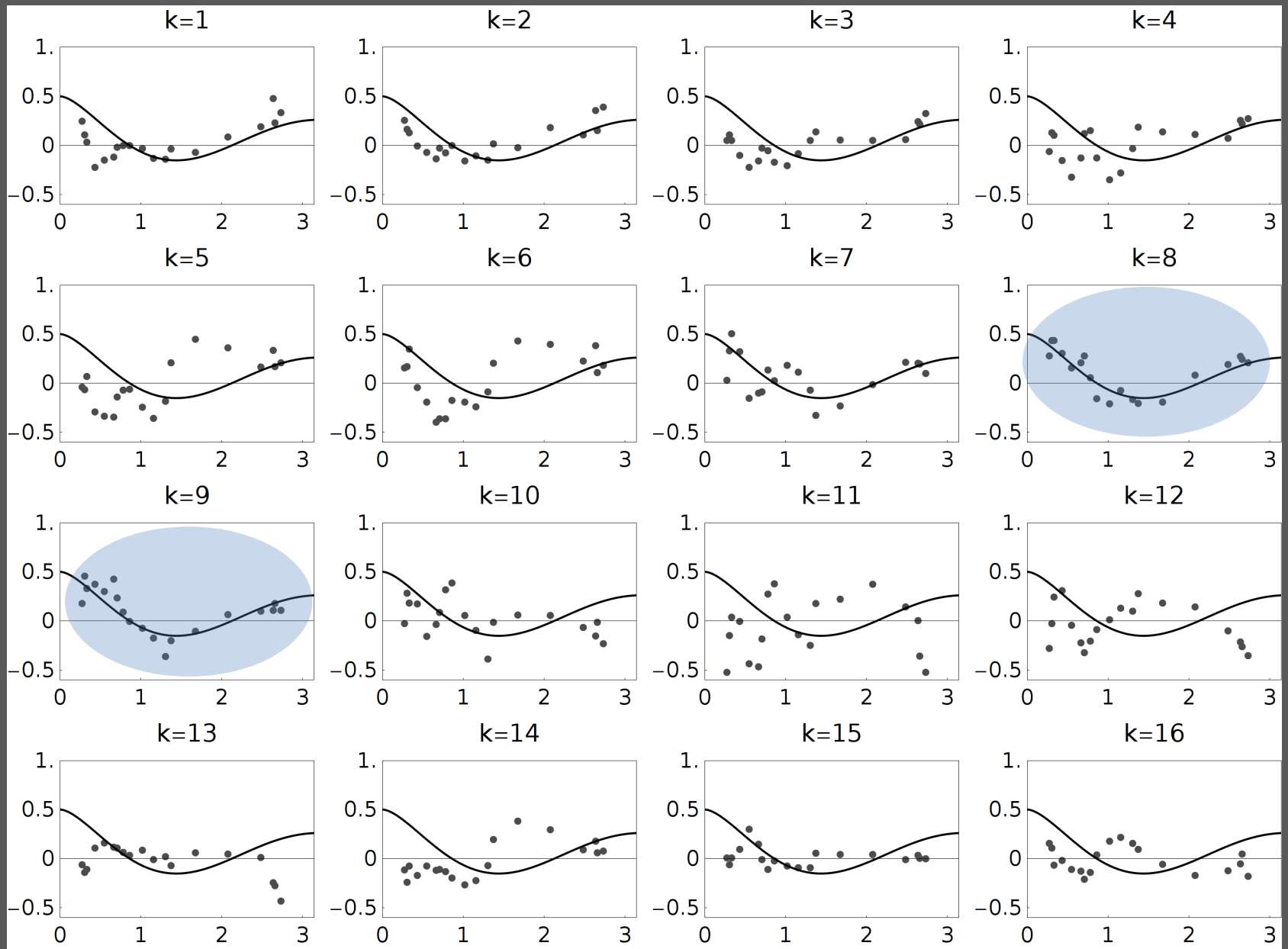
Computer simulation shows the influence of GW on the pulsar spin frequency. 1000 pulsars were put uniformly on the sky. Change of pulsar spin frequency is shown by color and size. The amplitude and direction of GW were set as random correlated functions of time. Pulsar spin frequency is spatially correlated in accordance with the two-point correlation function. Detection of GW is based on this principle.

Numerical simulation

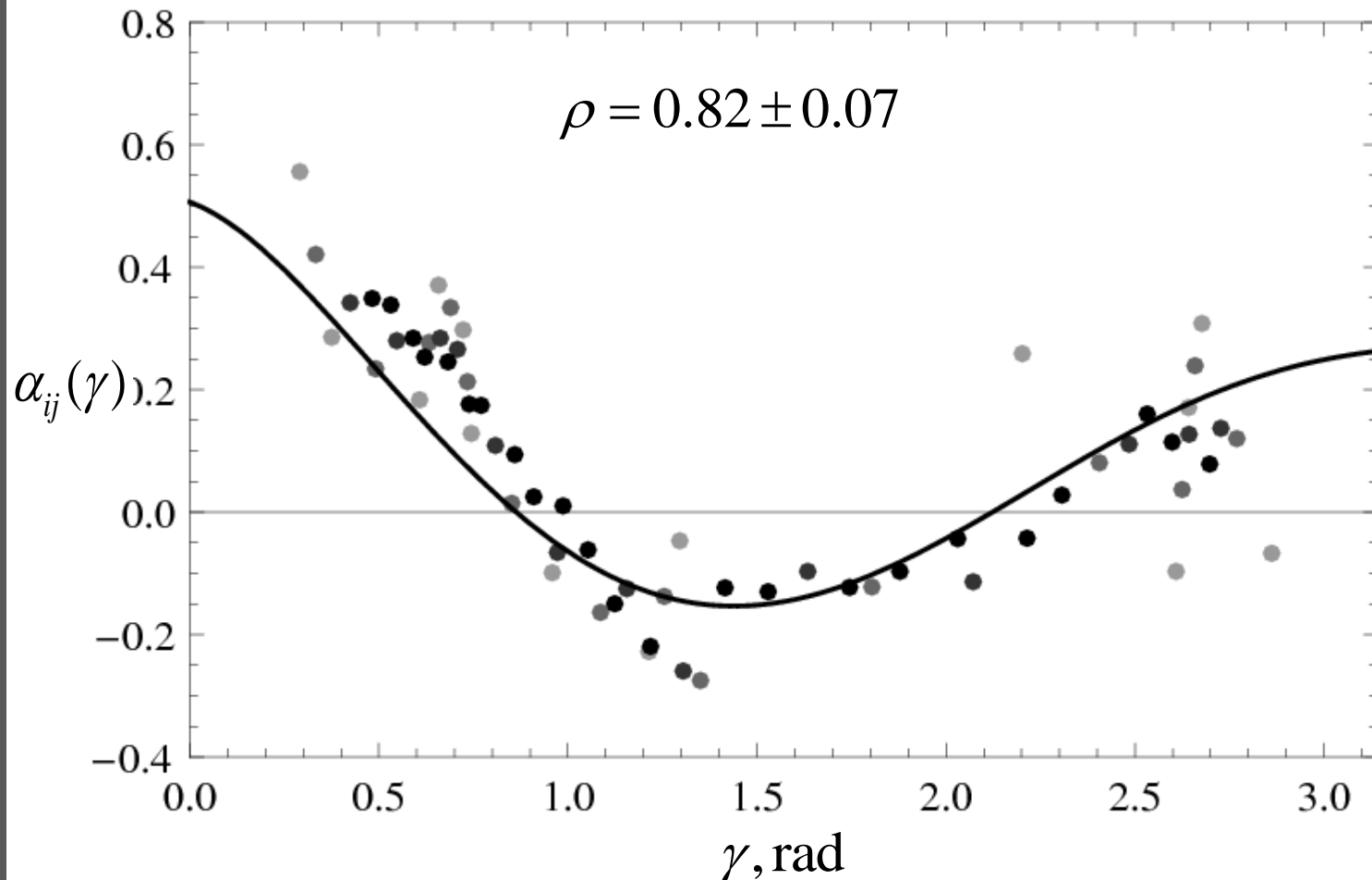


The theoretical two-point correlation function $\alpha_{ij}(\gamma)$ and results of computer simulation. Pulsar coordinates were taken the same with real pulsars. 6 pulsars and 50 trials (length of time series) allow to detect $\alpha_{ij}(\gamma)$ at the signal to noise ratio SNR=10.

Results



Results



Two-point correlation function (smoothed by 2-5 points) for 8th SSA-component. The probability that this correlation occurred by chance is $\Pr(\rho = 0.82, M = 15) \simeq 10^{-4}$.

A.Rodin, AIP Conference Proceedings, Volume 1357, pp. 81-84 (2011), [arXiv:1012.3038v1](https://arxiv.org/abs/1012.3038v1)

A.Rodin, Astronomy Reports, Volume 55, Issue 2, pp.132-141 (2011), [arXiv:1101.0063v1](https://arxiv.org/abs/1101.0063v1)

Discussion

The correlation amplitude $A=0.5$ mcs and time interval 6 yr produce the estimation of $\Omega_g = \rho / \rho_c \simeq 3 \cdot 10^{-9} h^{-2}$, where

$$\rho = \frac{243\pi^3}{416G} A^2 f^4 \quad \text{-- energy density of the monochromatic gravitational wave (Kaspi, Taylor, Ryba, 1994)}$$

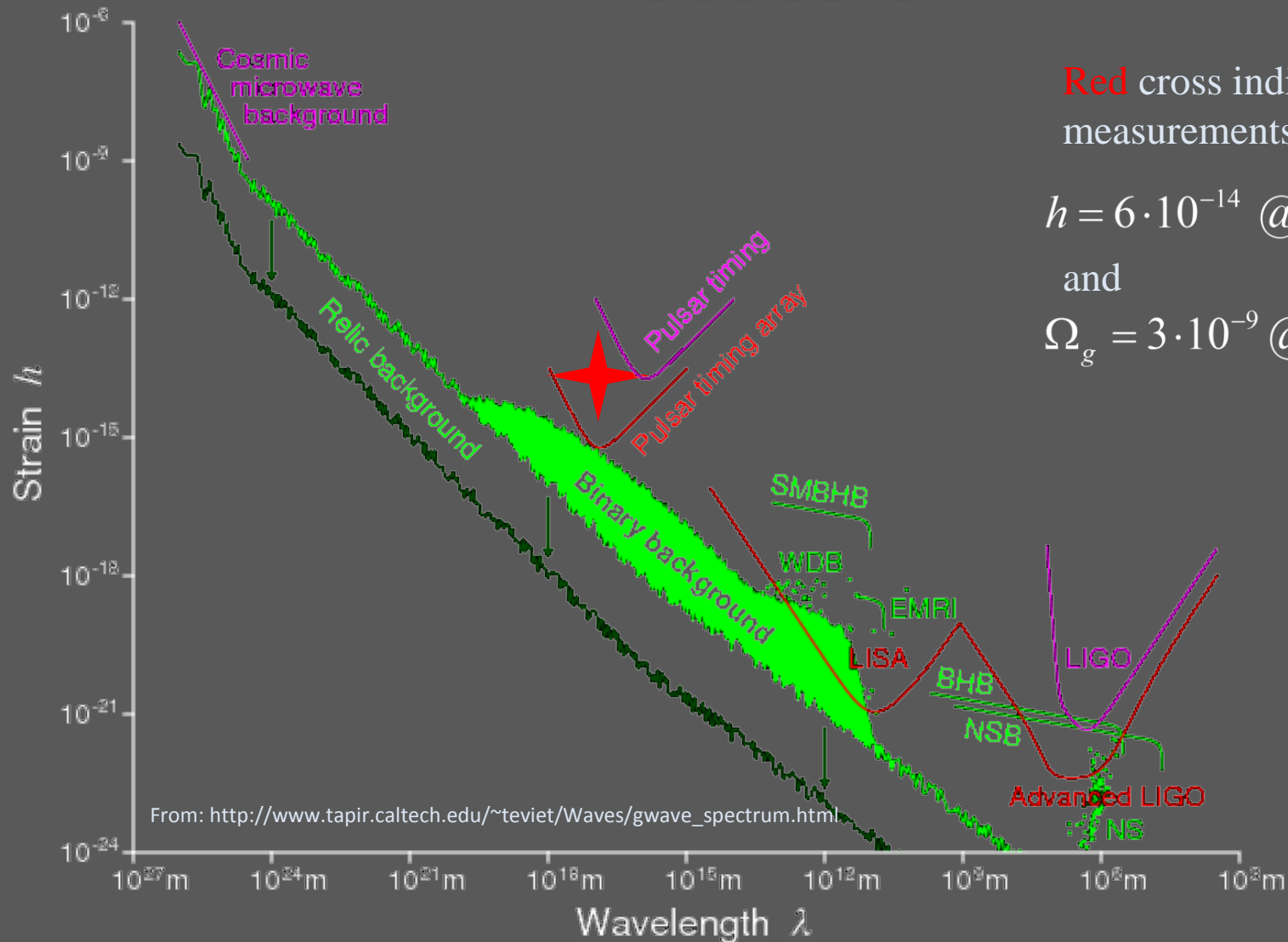
$$\rho_c = \frac{3H_0^2}{8\pi G} \quad \text{-- the Universe closure density}$$

$$h = \frac{H_0}{100 \frac{\text{km/s}}{\text{Mpc}}}$$

The correlation amplitude $A=0.5$ mcs in terms of dimensionless amplitude of the GW produces the value $h \simeq 6 \cdot 10^{-14}$.

The expected upper limits for the gravitational-wave background mentioned in many studies gives $\Omega_g h^2 < 10^{-10}$ (e.g. D. R. Lorimer, Living Rev. Relativ. **11**, 8 (2008)).

Discussion



Red cross indicates our measurements:

$$h = 6 \cdot 10^{-14} @ \lambda = 6 \cdot 10^{16} \text{ m}$$

and

$$\Omega_g = 3 \cdot 10^{-9} @ f = 5 \cdot 10^{-9} \text{ Hz}$$

Gravitational wave spectrum

Discussion

DM variations would be another important source of timing noise and, if not corrected, would result in variations of time of arrivals similar to that caused by gravitational waves.

However it is difficult to suppose that DM variations from different pulsars are correlated in GW manner.

The common source of such correlated variations would be heliosphere filled by solar wind. The overall shape of the heliosphere is controlled by the interstellar medium, through which it is traveling with the Sun, and the shape of the heliosphere is not perfectly spherical.

“Dispersion Measure Variations and their Effect on Precision Pulsar Timing”

(You et al, MNRAS, Volume 378, Issue 2, pp. 493-506)

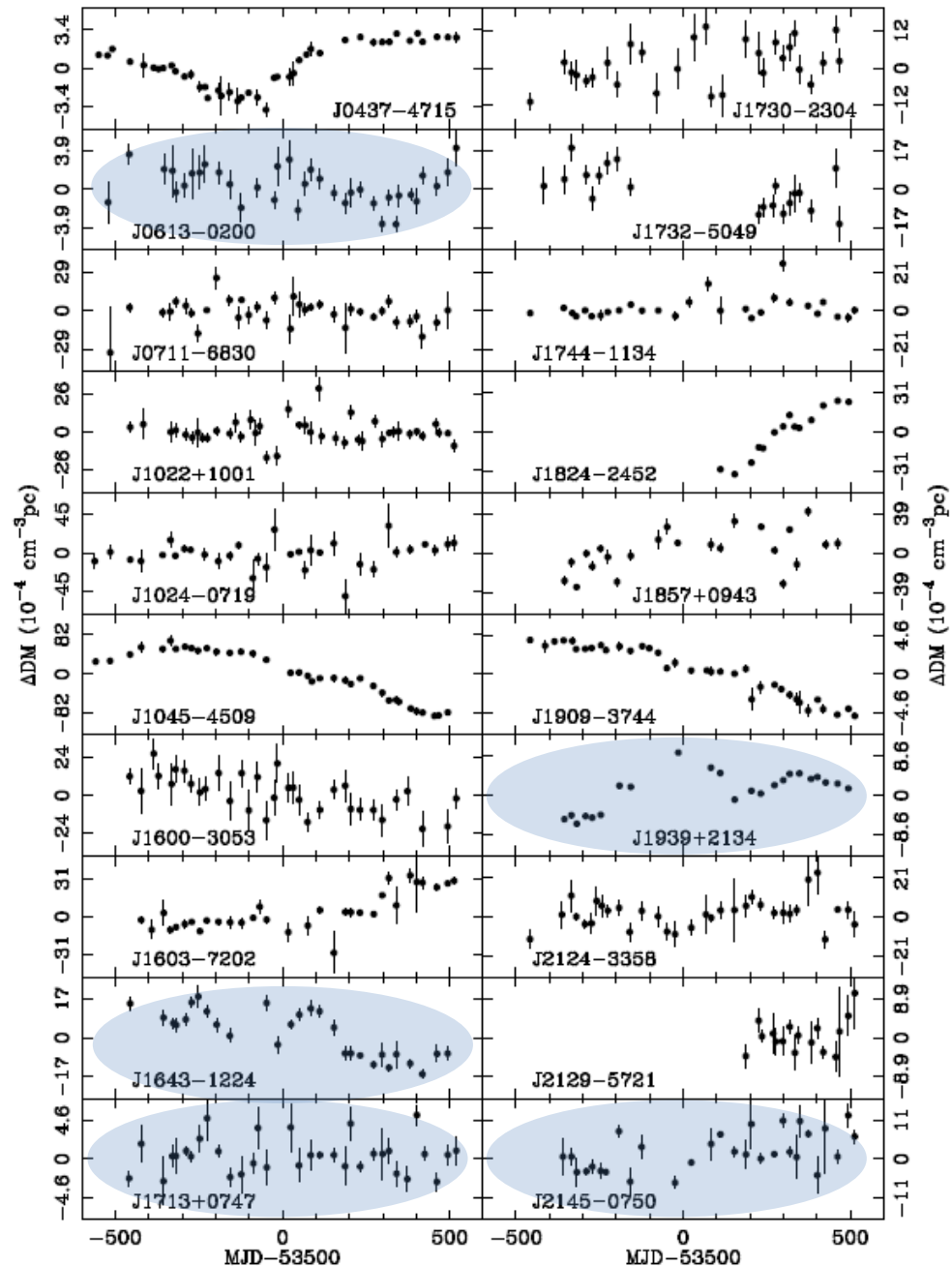
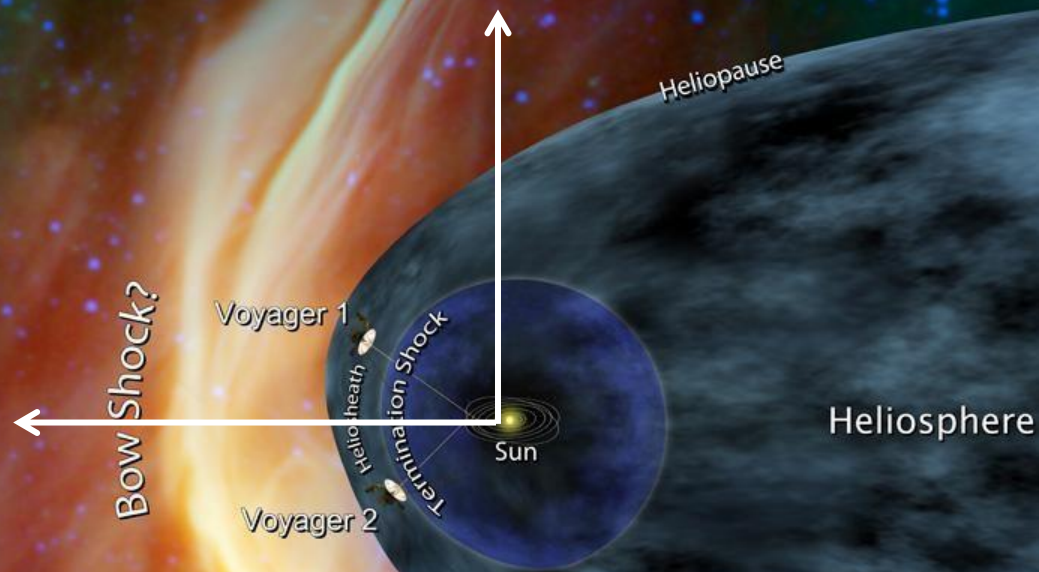


Figure 2. DM variations of 20 millisecond pulsars. Note a ΔDM of $10^{-4}\text{cm}^{-3}\text{pc}$ corresponds to time delays at 10 cm of 43 ns, at 20 cm of 212 ns and at 50 cm of 884 ns.

Discussion

Time delay 0.5 mcs @ frequency 610 MHz corresponds to $\Delta DM = 4.5 \cdot 10^{-5} \text{ cm}^{-3} \text{ pc}$
or electron concentration $\Delta n_e \approx 9 \text{ cm}^{-3}$.



From: http://www.nasa.gov/mission_pages/voyager/voyager-20071210.html

Artist's view of the heliosphere deformed due to motion of the Sun through the interstellar gas. When we observe pulsars we scan heliosphere at the different directions. Since the shape of the heliosphere is not spherical this may result in the same spatial correlation similar to that produced by gravitational waves.

Conclusion

1. Detected is an statistically significant effect similar to that predicted for stochastic GW background.
2. Correlation amplitude $A=0.5$ mcs and time interval 6 yr produce the estimation of $\Omega_g = \rho / \rho_c \simeq 3 \cdot 10^{-9} h^{-2}$ at frequency $f = 5 \cdot 10^{-9}$ Hz.
3. Alternative explanation of the revealed effect would be quadruple signature in a model of the electron density of the solar wind. Difference of electron concentration 9 cm^{-3} is sufficient value for describing the detected effect.
4. Additional theoretical criteria for detection of GW are required (detection of the signature may not signify detection of GW).

Author expresses a gratitude to personally Prof. Maxim Khlopov
for opportunity to give this lecture.

Thank you for attention!